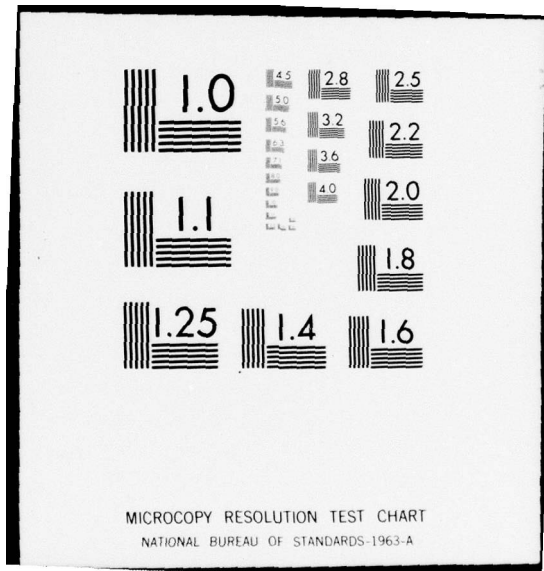


AD-A051 226 FLORIDA UNIV GAINESVILLE DEPT OF MATERIALS SCIENCE --ETC F/G 11/6
APPLICATION OF EXPERIMENTAL POURBAIX DIAGRAMS TO PREDICTION OF --ETC(U)
JAN 78 E D VERINK N00014-75-C-0820
UNCLASSIFIED NL

1 of 1
AD
A051226



END
DATE
FILMED
4 -78
DDC



MICROCOPY RESOLUTION TEST CHART
NATIONAL BUREAU OF STANDARDS-1963-A

AD A 051 226

12

9 FINAL REPORT

to the

OFFICE OF NAVAL RESEARCH

on Contracts

15 N-00014-75-C-0820
N-00014-68-A-0173-0015
and N-00014-68-A-0173-0003

6 APPLICATION OF EXPERIMENTAL POURBAIX DIAGRAMS TO
PREDICTION OF LOCALIZED CORROSION, DEALLOYING AND
STRESS CORROSION CRACKING OF ENGINEERING ALLOYS

AD NO. FILE COPY
DDC

11 12 Jan 78
12 19P

DDC
RECEIVED
MAR 16 1978
RECEIVED
A

10 Submitted by
Dr. Ellis D. Verink, Jr.
Department of Materials Science and Engineering
University of Florida
Gainesville, Florida 32611

January 12, 1978

DISTRIBUTION STATEMENT A
Approved for public release;
Distribution Unlimited

408 174

JOC

Introduction

This is the Final Report of Research under Contract N-00014-75-C-0820, entitled "Application of Experimental Pourbaix Diagrams to Prediction of Localized Corrosion, Dealloying and Stress Corrosion Cracking of Engineering Alloys."

The University of Florida greatly appreciates the support provided by the Office of Naval Research both to the Department of Materials Science and Engineering and to the eleven graduate students who received (at least partial) support.

Listed below is a summary of major accomplishments. Underlying all of these is a philosophy that there is a strong obligation to make corrosion research more cost-effective by providing a framework of theory and practice which will give a capacity for predicting corrosion behavior of engineering alloys at minimum cost in research time or resources.

The relatively heavy demand from both U.S. and foreign laboratories for reprints of a number of the papers and particularly for the computer program for complex Pourbaix Diagrams indicates that the work has received international attention.

Summary Listing of Major Accomplishments

Following is a list of research accomplishments due in whole or part to support by the Office of Naval Research through Contracts N-00014-75-C-0820, N-00014-68-A-0173-0015 and N-00014-68-A-0173-0003:

1. Development of an electrochemical method for assessing the influence of alloy additions on the corrosion behavior of alloys. (Three dimensional Pourbaix Diagrams, potential/pH/composition.) (1,3,5,7,8,11,12,26)*
2. Refined and extended the method for predicting the effect of alloy additions on the kinetics of corrosion reactions for alloys of a family. (Inclusion of corrosion rate "trajectories" on experimental potential/pH diagrams.) (2,3,5,8,12,15,19,26)
3. Developed a laboratory method for evaluating the influence of crevices on corrosion behavior of alloys and on the chemistry of the occluded cell formed by the crevice. (4,8,11,14,15,16,17,19,20,23,24,26)
4. Provided electrochemical elucidation of the mechanisms of dealloying for Cu-Zn alloys and developed a procedure for predicting when dealloying is likely (thermodynamically). (2,6,9,13,25,26)
5. Suggested a basis for predicting the limiting electrode potential and pH in occluded cells. The availability of such information facilitates design of simple experiments which reflect the effect of time-dependent chemical changes. (14,20,23,24)
6. Developed and made generally available a computer program for calculation of Equilibrium Pourbaix Diagrams for complex chemical systems. The availability of this program facilitates design of critical experiments. (21,22)

*Numbers in parentheses refer to publications listed on pages 5-8 hereof.

7. Computerized the estimation of thermodynamic data for ions at elevated temperatures using the Criss and Coble technique. (21,22)
8. Applied digital data manipulation techniques to improve the reliability of polarization data. (27)
9. Published sixteen (16) scientific papers in scholarly journals.
10. Provided partial or full support for eleven (11) Master's Degree graduates, one (1) Engineer Degree graduate and three (3) Ph.D. graduates. Five of the Master's Degrees were with thesis.
11. During the final year initiated preliminary research utilizing ring-disc electrode techniques in the study of dealloying.
12. Completed characterization of apparatus for development of elevated-temperature potential/pH diagrams and, with the help of the computer, selected the test conditions for a research program which will compare thermodynamic predictions with experimental results.

List of Graduate Students

Following is a list of graduate students who received all or part of their financial support from the Office of Naval Research on Contracts N-00014-75-C-0820, N-00014-68-A-0173-0015 or N-00014-68-A-0173-0003:

Master's Degree

*R. H. Heidersbach, Jr.

*J. N. Snodgrass

T. S. Lee, III

K. D. Efird

R. L. Cusumano

P. A. Parrish

*K. K. Starr

J. M. Bowers

*W. C. Fort, III

*I. D. Blecker

*M. H. Froning

Ph.D. Degree

R. H. Heidersbach, Jr.

K. K. Starr

W. C. Fort, III

Engineer Degree

M. H. Froning

*non-thesis

List of Publications, Theses and Dissertations

Following is a list of publications, theses and dissertations produced with Office of Naval Research support under Contracts N-00014-68-A-0173-0003, N-00014-68-A-0173-0015 and N-00014-75-C-0820:

1. P. A. Parrish, "Use of Experimentally Determined Pourbaix Diagrams to Elucidate the Role of Iron in the Passive Behavior of Copper-Rich Alloys Containing Nickel," M.S. Thesis, 1970.
2. E. D. Verink and P. A. Parrish, "Use of Pourbaix Diagrams in Predicting Susceptibility to Dealloying Phenomena," *Corrosion* 26, No. 5 (May 1970) 214.
3. E. D. Verink, Jr., "Construction of Pourbaix Diagrams for Alloy Systems with Special Application to the Binary Fe-Cr System," A. D. 740394, June 10, 1970.
4. K. D. Efird, "Crevice Corrosion of Copper-Nickel Alloy and Its Relationship to the Experimental Pourbaix Diagram," M.S. Thesis, 1970.
5. E. D. Verink and M. Pourbaix, "Use of Electrochemical Hysteresis Techniques in Developing Alloys for Saline Exposures," presented at Annual Meeting NACE, Chicago, Illinois, March 1971; *Corrosion* 27, No. 12 (1971).
6. R. H. Heidersbach, "The Dezincification of Alpha and Beta Brasses," Ph.D. Dissertation, 1971.
7. R. L. Cusumano, "The Establishment of a Three-Dimensional (potential/pH/composition) Diagram for Binary Fe-Cr Alloys in 0.1 Molar Chloride Solution," M.S. Thesis, 1971.
8. T. S. Lee, III, "The Use of Experimentally Determined Potential vs. pH Diagrams to Elucidate the Influence of Solute Additions on the Passive Behavior of Binary Cu-Ni Alloys in Solutions With and Without Chloride," M.S. Thesis, 1972.

9. E. D. Verink and R. H. Heidersbach, "Evaluation of the Tendency for Dealloying in Metal Systems," Localized Corrosion -- Cause of Metal Failure, STP 516 (1972) American Society for Testing Materials (ASTM), Philadelphia, Pennsylvania.
10. E. D. Verink, T. S. Lee, III and R. L. Cusumano, "Influence of Prior Electrochemical History on the Propagation of Localized Corrosion," Corrosion 28, No. 9 (1972).
11. E. D. Verink, "Applications of Electrochemical Hysteresis Methods in Assessing the Corrosion Behavior of Alloys," Proc. of the 5th Int'l. Congress on Metallic Corrosion, Tokyo, Japan, 1972.
12. E. D. Verink and T. S. Lee, III, "Influence of Minor Alloy Additions on the Passive Behavior of Binary Cu-Ni Alloys," Proceedings of 3rd Int'l. Conf. on Materials for the Sea, Gaithersburg, Maryland, October 1972.
13. R. H. Heidersbach, Jr. and E. D. Verink, Jr., "The Dezincification of Alpha and Beta Brasses," Corrosion 28, No. 11 (1972).
14. J. M. Bowers, "Crevice Corrosion of a 70-30 Chromium Modified Cupronickel and Its Relationship to the Experimental Pourbaix Diagram," M.S. Thesis, 1973.
15. K. K. Starr, "The Significance of the Protection Potential for Fe-Cr Alloys at Room Temperature," Ph.D. Dissertation, 1973.
16. W. C. Fort, III, "Mechanisms and Inhibition of Dealloying in Alpha Brass," Ph.D. Dissertation, 1975.
17. M. Pourbaix, J. V. Muylder, A. Pourbaix and E. D. Verink, "Etudes Electrochimiques Concernant les Corrosions en Cellules Occluses C.C.O. et Protection Contre ces Corrosions: Corrosion par Piqures, Corrosion Caverneuse, Corrosion Fissurante sous Tension, Corrosion Selective D'Alliages. Applications au fer et Aux Aciers, au Cuivre, aux Cupro-

- nickels et aux Laitons," *Electroanalytical Chemistry and Interfacial Electrochemistry* 62 (1975) 219-29.
18. R. E. Hummel, E. D. Verink, Jr. and C. W. Shanley, "Use of Electrochemical Techniques in Combination with Differential Reflectometry to Elucidate Experimental Pourbaix Diagrams," presented at the Int'l. Congress on Metallic Corrosion, December 1975, accepted for publication in Proceedings.
 19. K. K. Starr, E. D. Verink, Jr. and M. Pourbaix, "The Significance of the Protection Potential for Fe-Cr Alloys at Room Temperature," *Corrosion* 32, No. 2 (February 1976) 47-51.
 20. E. D. Verink, Jr., K. K. Starr and J. M. Bowers, "Chemistry of Crevice Corrosion as Observed in Certain Cu-Ni and Fe-Cr Alloys," *Corrosion* 32, No. 2 (February 1976) 60-64.
 21. M. H. Froning, "A Computer Program for Calculation of Potential-pH Diagrams of Metal-Ion-Water Systems," Engineer Degree, 1976.
 22. M. H. Froning, M. E. Shanley and E. D. Verink, Jr., "An Improved Method for Calculation of Potential-pH Diagrams of Metal-Ion-Water Systems by Computer," *Corrosion Science* 16 (1976) 371-77.
 23. C. M. Chen, M. H. Froning and E. D. Verink, Jr., "Crevice Corrosion and Its Relationship to Stress-Corrosion Cracking," Stress Corrosion -- New Approaches, STP 610 (1976) American Society for Testing Materials (ASTM), Philadelphia, Pennsylvania.
 24. K. D. Eford and E. D. Verink, Jr., "The Crevice Protection Potential for 90-10 Copper-Nickel," *Corrosion* 33, No. 9 (1977) 328.
 25. W. C. Fort, III and E. D. Verink, Jr., "Elucidation of the Mechanism of Dezincification by Auger Electron Spectroscopy in Combination with Electrochemical Methods," Proc. of the 4th Int'l. Congress on Marine Corrosion and Fouling, June 14-19, 1976, published 1977.

26. E. D. Verink, Jr., "Applications of Electrochemical Techniques in the Development of Alloys for Corrosive Environments," Electrochemical Techniques for Corrosion, NACE, Houston, Texas, 1977, Library of Congress No. 77-71054.
27. S. R. Bates, P. F. Johnson and E. D. Verink, "Computerized Methods for Polarization Measurements," to be presented at the 1978 Electrochemical Society Meeting to be held in Seattle, Washington in May 1978.

Technical Reports and Renewal Proposals

During the term of Contract N-00014-68-A-0173-0003 quarterly reports were submitted for inclusion in the Office of Naval Research report to Advanced Research Projects Agency (ARPA). In succeeding years under Contracts N-00014-68-A-0173-0015 and N-00014-75-C-0820 annual renewal proposals consisted of progress reports describing the status of on-going research, a research plan for the succeeding year and copies of publications, theses and/or dissertations generated during that year. The title, "Development of Experimental Pourbaix Diagrams for the Prediction of Corrosion Behavior of Alloys," remained the same from initiation in 1968 through the end of 1975. The final renewal proposal (December 1, 1975) was entitled "Application of Experimental Pourbaix Diagrams to Prediction of Localized Corrosion, Dealloying and Stress Corrosion Cracking of Engineering Alloys."

Current Year

A paper by K. D. Eford and E. D. Verink entitled "The Crevice Protection Potential for 90-10 Copper-Nickel" appeared in Corrosion Magazine 33, No. 9 (1977) 328. A copy is attached herewith. An extended abstract of a paper describing the computer control of electrochemical measurements and the use of computerized methods of data manipulation has been submitted to the Electrochemical Society for the May 1978 meeting. A copy of this abstract also is attached.

The Crevice Protection Potential for 90-10 Copper Nickel^{*}

K. D. EFIRD^{*} and E. D. VERINK, JR.^{**}

Abstract

The potential and pH variations for a simulated "crevice" on 90-10 Cu-Ni in 0.1M NaCl at pH 10.3 were determined for a range of external potentials, and related to the experimental potential-pH diagram for the alloy in 0.1M NaCl. The range of values of steady state potential and pH for "crevice" samples undergoes a discontinuity at an external potential of 0.140 ± 0.010 volts (SHE). The electrode potential at which this discontinuity occurs has been called the "crevice protection potential". At potentials more noble than the crevice protection potential, the metal in the crevice corrodes actively, and the occluded cell electrolyte becomes more acid. At more active potentials, the metal in the crevice passivates, and the occluded cell electrolyte becomes more alkaline. This crevice protection potential corresponds closely to the potential of the intersection of the "corrosion region" on the experimental potential-pH diagram and the locus of the primary passivation potential as a function of pH for the alloy. Cautiously, this concept might be applied to all copper base alloys exhibiting "copper type" potential-pH diagrams.

Crevice corrosion is generally attributed to the action of concentration cells,¹⁻³ with oxygen or metal ion concentration cells,⁴ and restricted ion transport and hydrolysis^{5,6} among the more widely accepted mechanisms. While research on crevice corrosion of stainless steels, titanium, and other passive alloys has been extensive, crevice corrosion studies on other alloys, particularly those which are not as highly passive, have not been as actively pursued.

The experimental potential-pH diagram for 90-10 Cu-Ni in 0.1M NaCl has been determined by Parrish,⁷ Lee,⁸ and Verink and Lee.⁹

The use of a divided test cell to study crevice corrosion, i.e., where the crevice sample is physically separated from the boldly exposed alloy, is not new. Pourbaix¹⁰ reported the potential-pH variation for a crevice on Armco iron exposed in 0.01M NaCl solution adjusted to pH 10 when the bulk of the sample was potentiostated within a selected range of potentials.

Experimental Procedure

The crevice corrosion characteristics of 90-10 Cu-Ni were investigated using a stirred, oxygenated solution of 0.1M NaCl at a bulk pH of 10.3 ± 0.1 , and a temperature of 25 C. The pH of the test solution was chosen to be well within the passive region for the alloy. The material used was commercially produced annealed sheet

^{*}Submitted for publication February, 1977.

^{*}The International Nickel Company, Inc., Francis L. LaQue Corrosion Laboratory, Wrightsville Beach, North Carolina.

^{**}Department of Materials Science and Engineering, University of Florida, Gainesville, Florida.

TABLE 1 - Composition of the
Alloy Used in the Crevice
Corrosion Experiments

Component	Wt%
Copper	Bal.
Nickel	9.98
Iron	1.46
Lead	0.02
Zinc	0.10
Manganese	0.43

with composition as given in Table 1. This was the same material that had been used to construct the experimental potential-pH diagram for the alloy.⁷⁻⁹

The test solution was made using triple distilled water and reagent grade chemicals. No buffer was used, therefore, the bulk solution pH was checked twice daily during an experiment, and adjusted as necessary by the addition of dilute sodium hydroxide or hydrochloric acid in 0.1M NaCl. The bulk solution was oxygenated using chemically pure oxygen which had been passed through 10% NaOH and distilled water before entering the test cell.

Sample preparation consisted of metallographic polishing through 600 grit SiC paper, rinsing in distilled water, ultrasonically

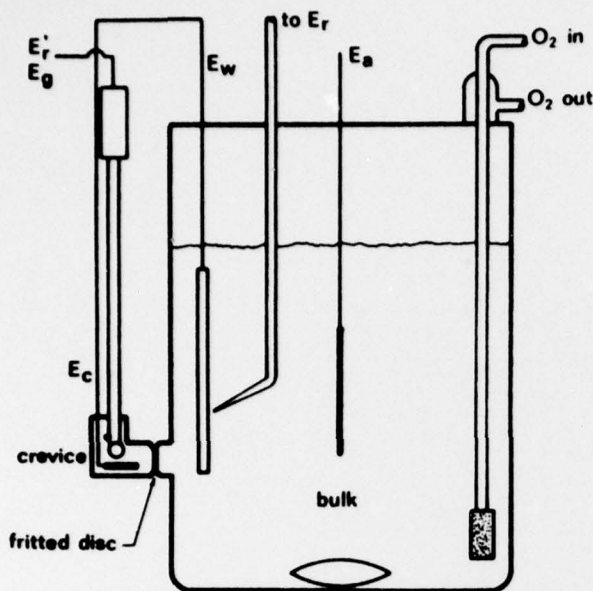


FIGURE 1 - The crevice corrosion test cell. E_c = crevice sample electrode, E_r' = crevice reference electrode, E_g = glass pH electrode, E_w = boldly exposed sample (working) electrode, E_r = open reference electrode, and E_a = Pt auxiliary electrode.

cleaning in a 50/50 mixture of reagent grade acetone and benzene, a second distilled water rinsing, and air drying. Areas of the sample that were not to be exposed were coated with a Tygon varnish, and the prepared sample was stored in a desiccator for 24 hours before exposure.

The corrosion cell used was divided so that the "crevice" and "open" areas were physically separated by a 4 micron porosity fritted glass disc sealed between the cells as diagramed in Figure 1. The open cell volume was 1000 ml, and the crevice cell volume was approximately 4 ml. The sample exposed in the open cell ("boldly exposed" sample) was 50 x 75 mm with an exposed area of 2000 mm², while the sample in the crevice cell ("crevice" sample) had an exposed area of 100 mm², giving a bold/crevice area ratio of 20:1.

The cell design, obviously, does not exactly duplicate an actual crevice on a material. However, it does include many of the important features of an occluded cell, with the added convenience of permitting experimental measurements to be made and solutions to be analyzed.

The top of the crevice cell was sealed with a rubber stopper, which had been drilled to accommodate the insulated connecting wire from the crevice sample (E_c) and a microcombination (glass:Ag/AgCl) electrode, providing a reference electrode for the crevice (E_r') as well as pH measurement (E_g). The boldly exposed sample (E_w) was electrically connected to the crevice sample. The boldly exposed sample potential was measured using a Luggin-Haber probe and salt bridge connected to a saturated calomel electrode (E_r). A bright platinum screen slightly larger than the boldly exposed sample surface served as an auxiliary electrode (E_a).

The electrode potential of the boldly exposed sample was controlled at a chosen (constant) potential using a Wenking model 68TA1 potentiostat. The crevice potential and pH were permitted to change in response to the reactions taking place. Detailed measurements of potential and pH were made using a Keithley model 602 electrometer with a pH adapter, and recorded using a strip chart recorder. The electrical schematic for the test system is shown in Figure 2.

The conditions in the crevice were assumed to have reached a steady state condition when the electrode potential of the crevice sample and pH in the crevice compartment remained constant for a 6 hour period. The time required for these conditions to be reached was generally of the order of 70 to 100 hours. After steady state

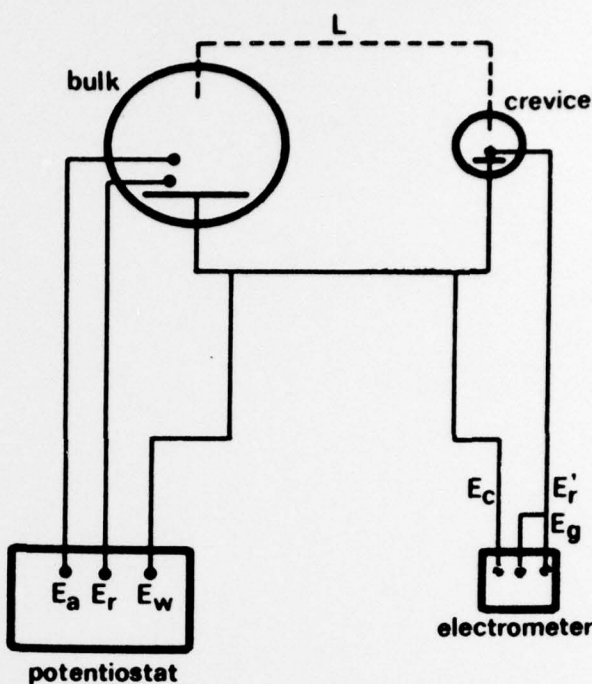


FIGURE 2 - Electrical schematic for the crevice corrosion test cell. L = liquid junction (through the fritted glass disc), E_a = Pt auxiliary electrode, E_r = open reference electrode, E_w = boldly exposed sample (working) electrode, E_c = crevice sample electrode, E_r' = crevice reference electrode, and E_g = glass pH electrode.

TABLE 2 - The Effect of External Potential on the Steady State Crevice Potential and pH in 0.1M NaCl at pH 10.3

Point ⁽¹⁾	External Potential [V (SHE)]	Crevice	
		Potential [V (SHE)]	pH
1	0.250	0.218	5.3
2	0.220	0.210	5.5
3	0.190	0.173	5.8
4	0.160	0.145	6.3
5	0.130	0.132	10.4
6	0.090	0.095	10.8
7	0.040	0.050	11.1
(2)	0.151	0.133	6.3

(1) Refers to point numbers in Figure 3.

(2) Freely corroding.

conditions were reached, the cell was disassembled, and the crevice solution and open solution were each titrated to determine their chloride ion concentration. The nature of corrosion in the crevice sample was observed and recorded, and the composition of the corrosion product was determined using X-ray diffraction techniques.

Results and Discussion

The potential and pH variations observed in the crevice compartment when a 90-10 Cu-Ni specimen was exposed in 0.1M NaCl initially at pH 10.3 are given in Table 2 for a range of external potentials. These data are plotted on the experimental potential-pH diagram for the alloy in Figure 3.

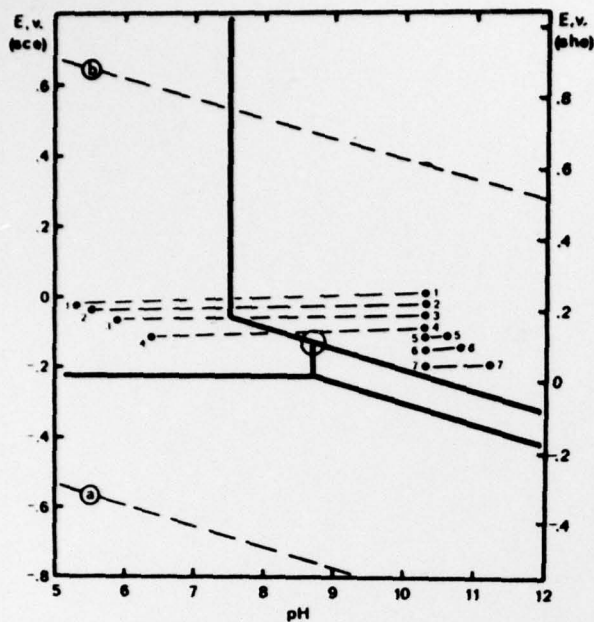


FIGURE 3 - The influence of external potential on the potential and pH characteristics of a crevice on 90-10 Cu-Ni. The numbers indicate simultaneous data for the crevice and the external surface. The intersection of the general corrosion region and the primary passivation line is circled for reference.

The steady state potential-pH curve for the crevice (Figure 4) undergoes a discontinuity within a narrow range of external potentials at 0.140 ± 0.10 volts (SHE). At external potentials more noble than this discontinuity, the crevice electrolyte acidifies and the electrode potential of the crevice sample becomes slightly active with respect to the external potential. Under these circumstances, the metal in the crevice corrodes by formation of a brown-red deposit overlain by a loose light green deposit. The brown-red deposit was identified by X-ray diffraction analysis as copper plus cuprous oxide, and the green deposit identified as cupric trihydroxychloride, with cupric hydroxide and cupric oxychloride possibly present.

At external potentials more active than the discontinuity, the pH of the crevice electrolyte increases and the electrode potential of the crevice sample becomes more noble than the external potential. The crevice metal is discolored slightly due to a thin passivating film which was too thin for positive identification by X-ray analysis. The slight change in color indicated that the stifling of attack was by a passivation reaction rather than a deactivation mechanism. Thus, the potential of discontinuity appears to be a dividing potential between corrosion and passivation of the crevice, and has been termed by the authors the "crevice protection potential".

The change in chloride ion concentration in the crevice is also a function of the relationship of the external potential to the "crevice protection potential" as shown in Table 3. When the electrode potential of the boldly exposed sample is more noble than the crevice protection potential, the chloride ion concentration within the crevice cell increases. When the electrode potential of the boldly exposed sample is more active than the crevice protection potential, the chloride ion concentration decreases slightly. Such changes in chloride ion concentration are explainable on the basis of cuprous ion complex formation with chloride ion and the resulting chloride ion activity gradient.

For example, when the metal within the crevice is corroding, cuprous ions produced in the corroding crevice readily react with chloride ions, forming the ionic complex CuCl_2^- . The result is an effective decrease in the chloride ion activity in the crevice, and a resulting net migration of chloride into the crevice. The chloride ion increase in the freely corroding crevice is two to three times greater

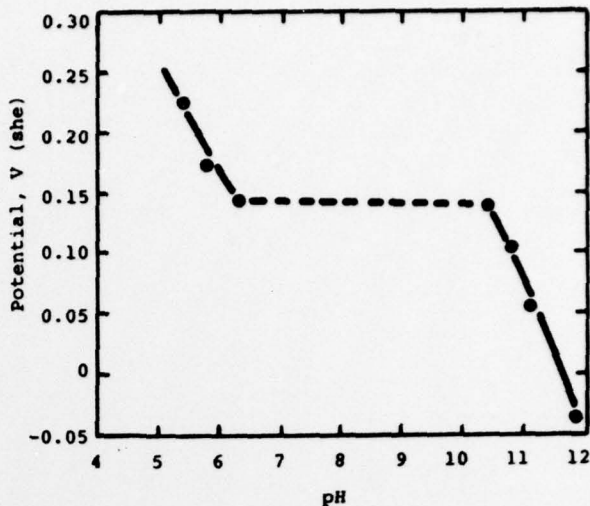


FIGURE 4 - Variation of pH in a crevice on 90-10 Cu-Ni at a range of potentials. The discontinuity occurs at 0.14 V (SHE).

TABLE 3 - The Effect of External Potential on the Change in Chloride Concentration in the Crevice in 0.1M NaCl at pH 10.3

Point ⁽¹⁾	External Potential [V (SHE)]	Crevice Change in Cl (Moles/l)
1	0.250	+0.005
2	0.220	+0.008
3	0.190	+0.006
4	0.160	+0.006
5	0.130	-0.001
6	0.090	0.0
7	0.040	-0.002
(2)	0.151	+0.016

(1) Refers to point numbers in Figure 3.

(2) Freely corroding.

than when an external potential is applied. In the polarized cell, electromigration of ions in response to the applied electric field acts in opposition to the activity gradient to effectively reduce the diffusion of chloride ions into the crevice volume over what would normally occur in a freely corroding system.

By contrast, when there is no corrosion in the crevice, there is no activity gradient and consequently no increase in chloride ion concentration occurs. The observed chloride ion concentration decreases are probably due to the electromigration effects mentioned above, and/or charge balance requiring the loss of chloride ion due to the generation of hydroxide ion in the cathodic crevice area.

The close proximity of the potential of the crevice discontinuity to the intersection of the general corrosion region and the primary passivation line (circled in Figure 3) indicates some significance for the primary passivation reaction to the protection of the crevice.

The effect of potentiostating the boldly exposed sample at potentials in various passive regions of the experimental potential-pH diagram was investigated using chronoamperometry (current density vs time). A 90-10 Cu-Ni sample was polarized above the primary passivation potential until the steady state current density was obtained. The potential was then stepped below the primary passivation potential.

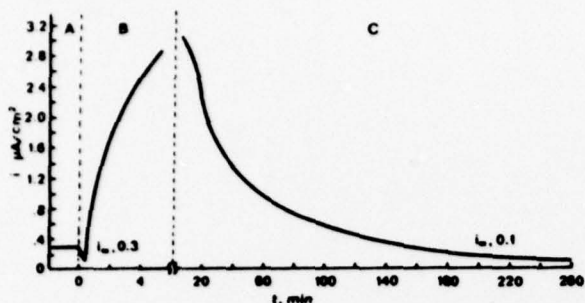
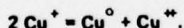


FIGURE 5 — Chronoamperometric curve for 90-10 Cu-Ni in 0.1M NaCl at pH 10.0. Section A is the steady state current density at a controlled potential of 0.110 V (SHE). At time zero, the potential was stepped to 0.040 V (SHE).

In Figure 5, the region marked "A" shows the steady state current density which was achieved after potentiostating a 90-10 Cu-Ni sample at 0.110 volts (SHE) in a solution of 0.1M NaCl at pH 10. At the time marked zero, the potential was instantaneously reduced to 0.040 volts (SHE). In region B, the current density increases from 0.3 $\mu\text{A}/\text{cm}^2$ for approximately 10 minutes, and subsequently decreases to 0.1 $\mu\text{A}/\text{cm}^2$ in 250 minutes. This behavior indicates that on polarizing from noble to active of the primary passivation potential a second film is formed, as indicated by the increase and subsequent decrease in current density, and that this new film is more protective than the initial film, as indicated by its significantly lower steady state current density.

The significance of the crevice protection potential on corrosion in a crevice is illustrated with the aid of Figure 6. When the material with a crevice present is at a potential "K" (more noble than the crevice protection potential), a passive film first begins to form. The local surface pH in the crevice drops to a pH such as "L", the lower pH limit for the passive region of the diagram, by production of hydrogen ions in the passivation reaction: $\text{M}^+ + \text{H}_2\text{O} = \text{MOH} + \text{H}^+$. The time period during which the pH changes from "K" to "L" is the initiation period for the activation of the crevice.

As the pH drops below "L", the crevice enters an active corrosion region. The film begins to break down and metal ion hydrolysis begins, further lowering the crevice pH. Corrosion continues and the pH drops due to metal ion hydrolysis, and, if the potential is below that of the Cu/CuCl reaction, copper redeposition can occur. The crevice reaches steady state at "M". Additional copper redeposition is probably due to the disproportionation reaction of cuprous ion:



This supposition is supported by the presence of cupric compounds in the crevice volume where oxygen was excluded.

When the alloy is at a potential "X" (more active than the crevice protection potential), the local crevice pH drops during passive film formation as in the previous case to a locus such as "Y" in Figure 6. However, in this case the primary passivation potential is reached at "Y" instead of an active corrosion region. The crevice is then repassivated by the formation of a second passive film, which has been shown to be more protective than the originally formed film that exists on the external surface.

When the repassivation in the crevice is complete, it is more noble than the external surface. As a result, the pH in the crevice increases until steady state is reached at "Z".

Conclusions

1. An experimental method has been developed for the detailed study of crevice corrosion mechanisms and effects using a simulated "crevice" sample and a "boldly exposed" sample in a 2 part cell of special design, which simulates many of the characteristics of an actual service, but facilitates experimental measurements.

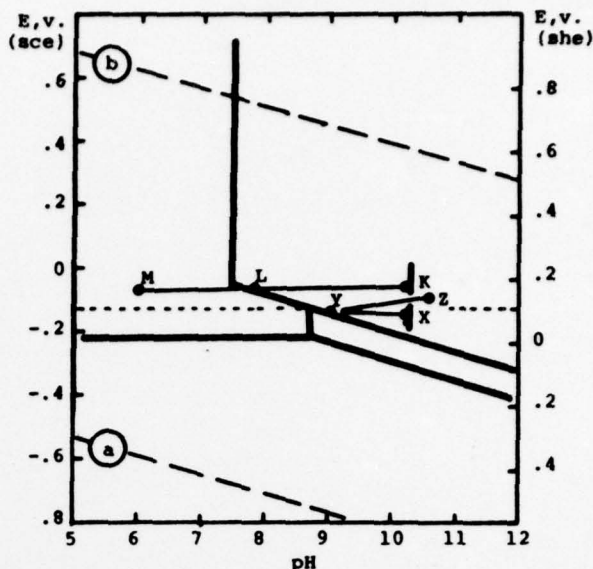


FIGURE 6 — The critical points during potential and pH changes occurring in a crevice at external potentials noble (K) and active (X) to the crevice protection potential. The broken line denotes the "crevice protection potential".

2. There is an electrode potential (for a boldly exposed sample) called the "crevice protection potential", which exists for certain copper base alloys. When the potential of the boldly exposed specimen is more active than this potential, the crevice is passive. When the potential of the boldly exposed specimen is more noble than this potential, crevice corrosion is active. This potential is related to passivation phenomena elucidated by the experimental potential-pH diagram for the alloy.

3. Since this crevice protection potential is dependent on the copper like nature of the potential-pH diagram, it is suggested that this concept might be applicable to all copper base alloys having the same general features in their experimental potential-pH diagram.

Acknowledgments

This research was conducted at the University of Florida, supported by the Advanced Research Project Agency, and administered by the Office of Naval Research, Washington, DC, and by the Office of Saline Water, Washington, DC.

References

1. R. J. McKay. Transactions of the Electrochemical Society, Vol. 41, p. 201-215 (1922).
2. R. J. McKay. Industrial and Engineering Chemistry, Vol. 17, p. 23-24 (1925).
3. U. R. Evans. Metallic Corrosion, Passivity, and Protection, Edward Arnold and Co., London (1946).
4. E. H. Wyche, L. R. Voight, and F. L. Laque. Transactions of the Faraday Society, Vol. 45, p. 683-693 (1949).
5. I. L. Rosenfeld and I. K. Marshakov. Corrosion, Vol. 20, p. 115t-125t (1964).
6. B. F. Brown. Corrosion, Vol. 26, p. 249-250 (1970).
7. P. A. Parrish. Master of Science Thesis, University of Florida (1970).
8. T. S. Lee, III, Master of Science Thesis, University of Florida (1972).
9. E. D. Verink, Jr. and T. S. Lee, III, Proceedings: 3rd International Congress on Marine Corrosion and Fouling, p. 241-263 (1972).
10. M. Pourbaix. Corrosion, Vol. 26, p. 431-438 (1970).
11. W. M. Latimer. Oxidation Potentials, 2nd ed., Prentice-Hall, Inc., Englewood Cliffs, NY (1961).

COMPUTERIZED METHODS FOR POLARIZATION MEASUREMENTS

S. R. Bates, P. F. Johnson, E. D. Verink
Department of Materials Science and Engineering
University of Florida, Gainesville, Florida 32611

Introduction

Methods of potention-kinetic measurements have been standardized under ASTM specification G5. Nonetheless, there is considerable uncertainty in the interpretation of such data. One source of uncertainty involves identification of the significant features of the resulting polarization curves where conventional methods are used. Computerization of the process should greatly simplify the generation of statistically significant data since use of computerized methods makes available to the corrosion scientist many of the powerful data-reduction techniques which have been found useful elsewhere.

Direct benefits include: (1) scrupulously reproducible polarization techniques resulting from mechanization of the process; (2) easy determination of the statistical limit of accuracy of the polarization data; (3) more accurate determination of features of polarization curves, E_{pp} , E_R , E_p , Tafel slope, etc.; (4) an internal test of the "quality" of the data; (5) elimination of noise, thereby facilitating the determination of points of inflection on the polarization curve; (6) (by use of a dummy load) the determination of the extent of and correction for instrumental error.

Experimental

Using a Princeton Applied Research Corp. scanning potentiostat model 173 with a universal programmer model 175, samples of 430 stainless steel were subjected to conditions described in ASTM specification G5 (potential range from -0.6 to 1.6 volts SCE in one normal sulfuric acid at $30^\circ\text{C} \pm 1^\circ\text{C}$). The equipment arrangement was similar to that shown in the specification.

The PAR scanning potentiostat and a universal programmer were used to generate the driving potential ramp. A digital control interface was constructed which systematically changed the potential by the selected voltage interval and then held the potential for a 10 second period of time before taking the next step. A current-digitizer-counter was used to convert the analog current to digital data suitable for transfer to a storage device. The data were subsequently plotted in the desired form.

The ASTM Standard specifies 50 millivolt steps. Since a step scanning procedure, if done manually, represents a tedious process, the choice of a 50 millivolt interval (rather than a much smaller interval) represents a compromise to reduce some of the tedium. Because of the versatility of the modified system employed in these experiments, we were not restricted to 50 millivolt increments but varied the magnitude of the voltage steps to illustrate the influence of this variable.

Figure 1 shows a computer-plotted polarization curve for data taken in 10 millivolt increments. The data fall within the envelopes of data shown in ASTM G5. However, analysis of the data showed that there are a number of statistically significant subtleties in the

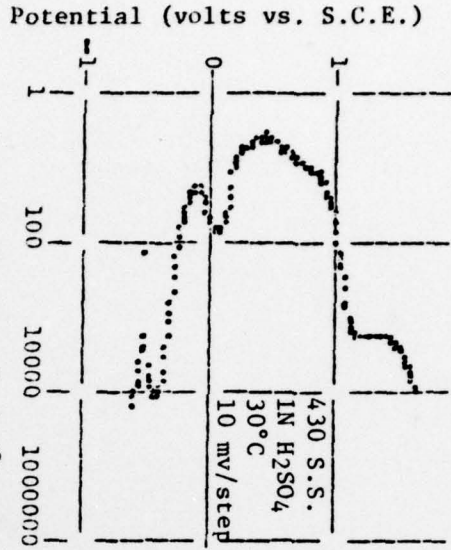
curve which have not heretofore been examined. It is not the purpose of this paper to deal with these subtleties or their significance at this time, but merely to point out that by use of computer techniques it is possible to find these subtle variations so that they may in time be studied. Figure 2 is an enlargement of the "active" region of Figure 1.

Figure 3 shows the first derivative of the data presented in Figures 1 and 2 and clearly shows various maxima and minima indicating limits of the straight line region as well as some fine "structure," indicating other possible processes. The ability to correlate features on the derivative curve with corresponding features on the polarization curve provides a strong verification of the quality of the data.

Figure 4 shows that the selected size of the voltage step-interval can influence the data. In Figure 4, step intervals of 5, 10 and 20 millivolts were used. With the computerized process the operator is not inconvenienced by selecting extremely small steps and thereby can optimize the test method to match the purpose of the test.

Conclusion

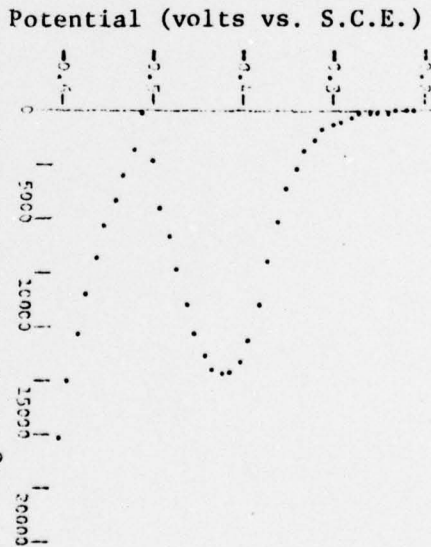
Computerizing of the generation of polarization curves offers important advantages. Computer storage provides an easy means for manipulating and displaying the data in a number of desirable forms. For example, it is simple to treat data statistically, calculate slopes, determine amount of charge passed, calculate areas of hysteresis loops, etc., all automatically. The internal controls which are implicit in the process make much simpler and more accurate the identification of significant features of polarization curves. Present results indicate that there are a number of subtleties in the polarization curve for 430 SS (for example) which may deserve more detailed study.



Current Density ($\mu\text{A}/\text{cm}^2$)
 Figure 1. Computerized Anodic Polarization Plot



Potential (volts vs. S.C.E.)
 Figure 3. Derivative of data presented in Figure 2



Current Density ($\mu\text{A}/\text{cm}^2$)
 Figure 2. Expanded view of the active region of Figure 1

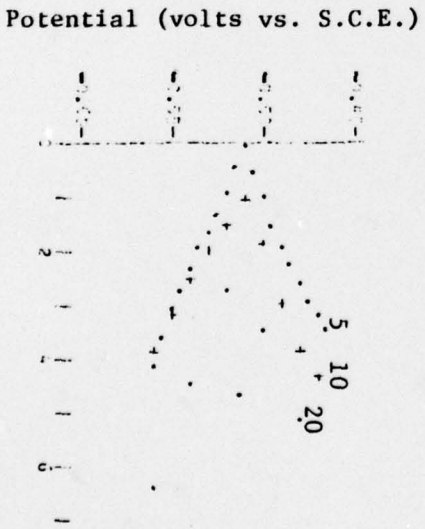


Figure 4. Effect of data acquisition interval on the shape of the polarization curve near $E_{\text{corrosion}}$